# Supplementary Information

## Limitations of polymer-based hole transporting layer for application in planar inverted perovskite solar cells

*Miloš Petrović,[a] Temur Maksudov,[a] Apostolos Panagiotopoulos,[ab] Efthymis Serpetzoglou,[cd] Ioannis Konidakis,[d] Minas M. Stylianakis,[a] Emmanuel Stratakis,[bd] Emmanuel Kymakis*[*,a]*

[a]*Department of Electrical & Computer Engineering, Hellenic Mediterranean University, Heraklion, 71410 Crete, Greece, Greece*

[b]*Department of Materials Science and Technology University of Crete Heraklion, 71003 Crete, Greece.*

[c]*Physics Department, University of Crete, 71003 Heraklion, Crete, Greece*

[d]*Institute of Electronic Structure and Laser (IESL), Foundation for Research and Technology−Hellas (FORTH), 71110 Heraklion, Crete, Greece.*

*Corresponding author:

Email: kymakis@staff.teicrete.gr

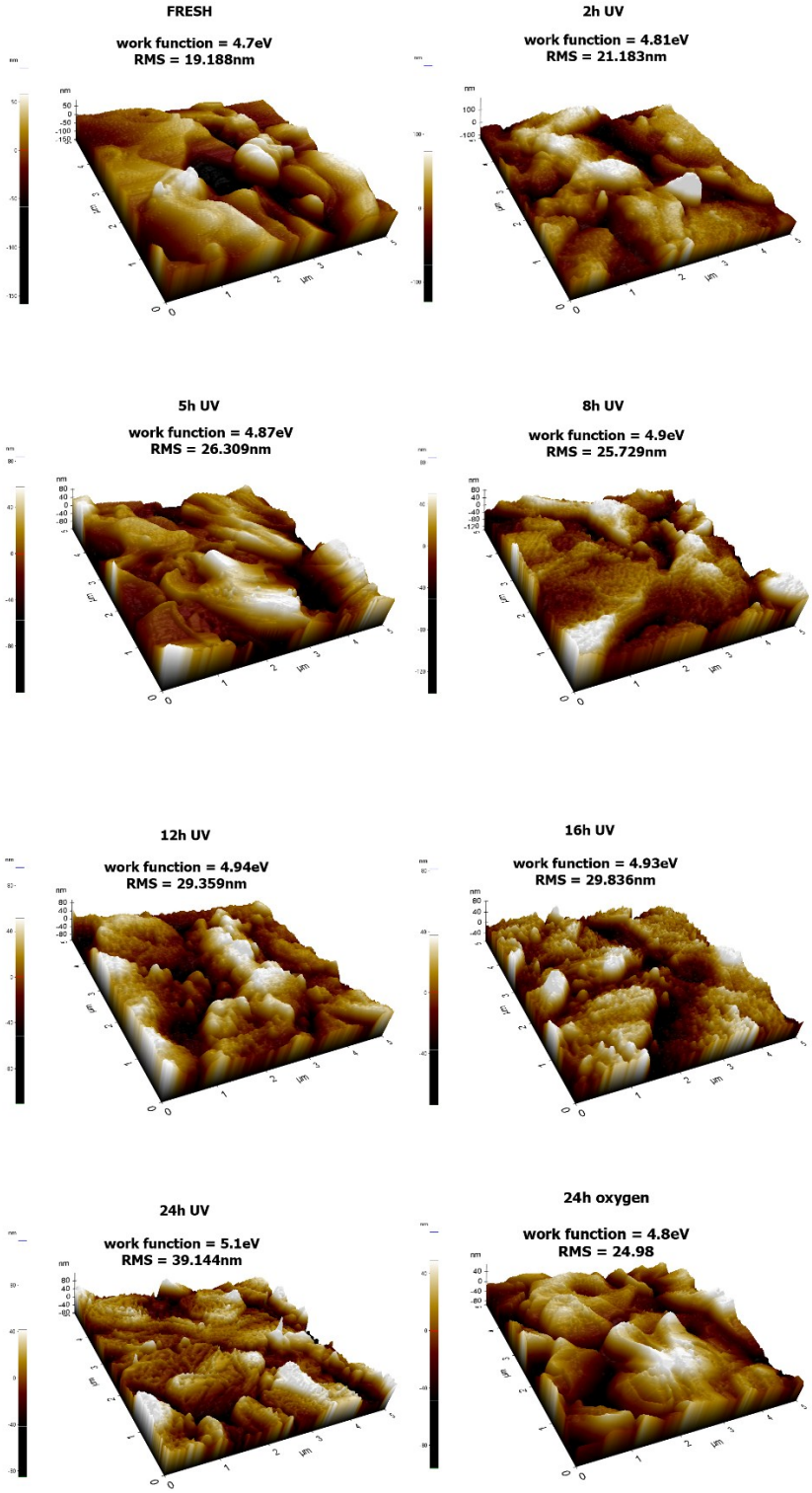


**Fig. S1.** AFM topography images of PTAA/MAPI bilayers resulting from various ageing conditions.

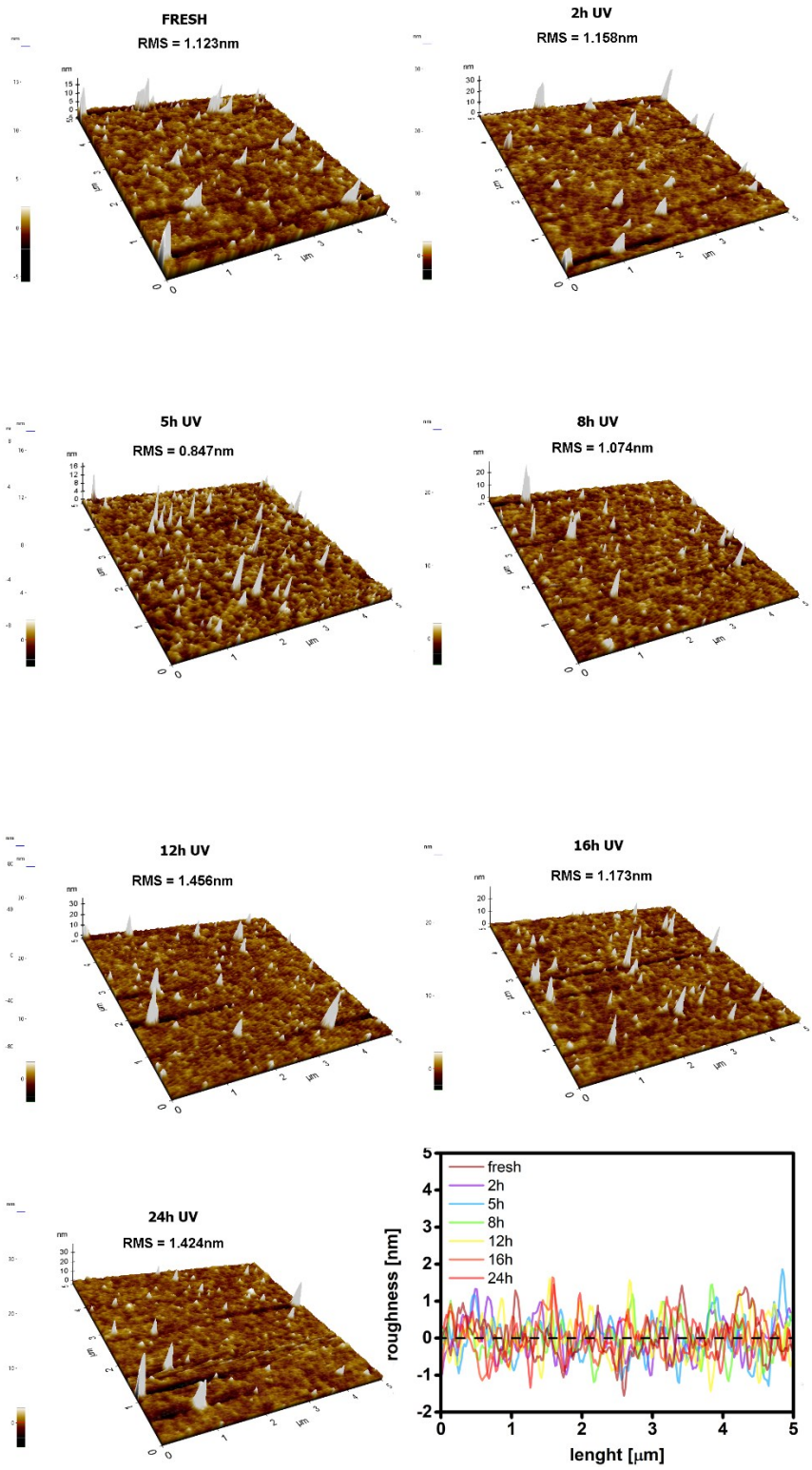


**Fig. S2.** AFM images of UV degraded PTAA films and corresponding roughness distribution.

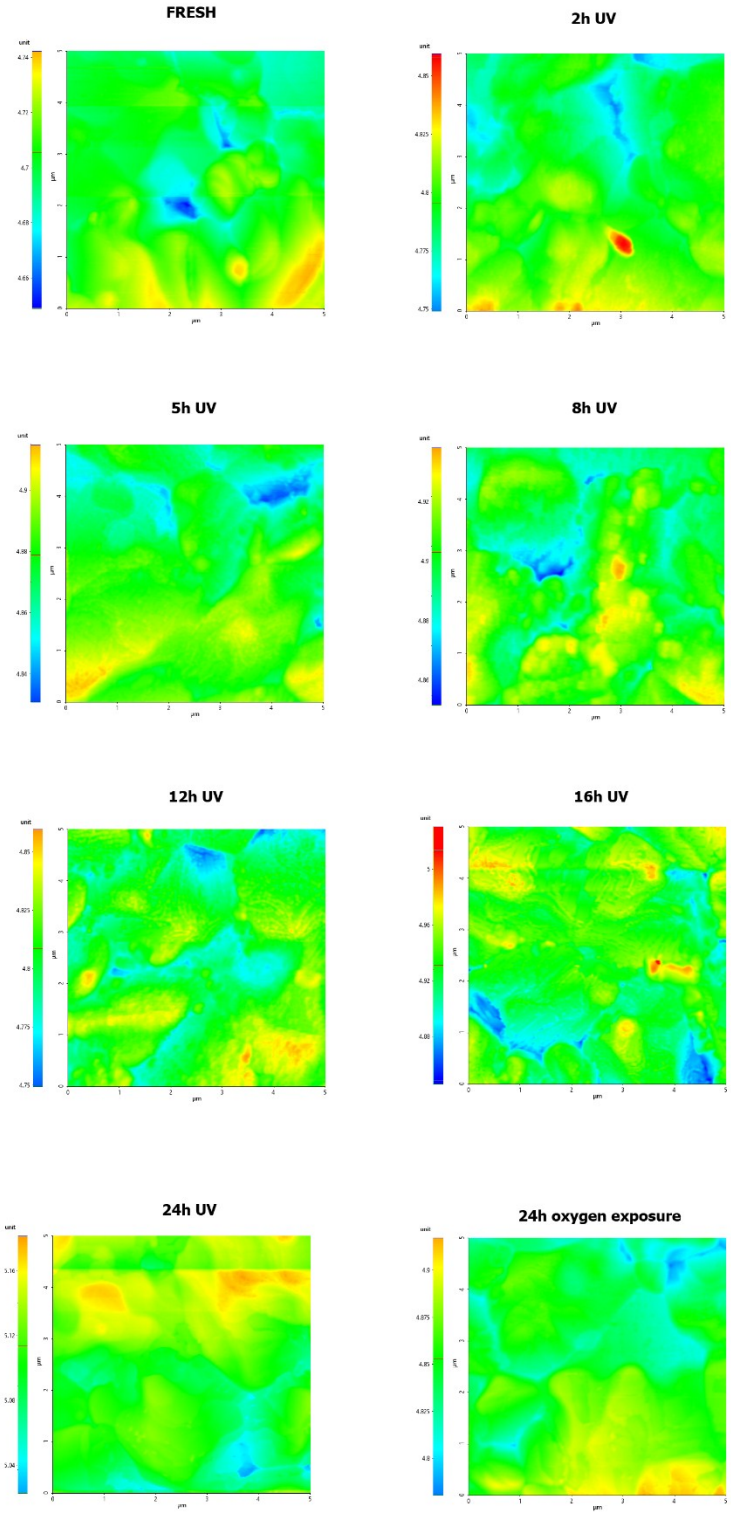


**Fig. S3**. Surface potential distribution of MAPI deposited over PTAA after various ageing periods and conditions.

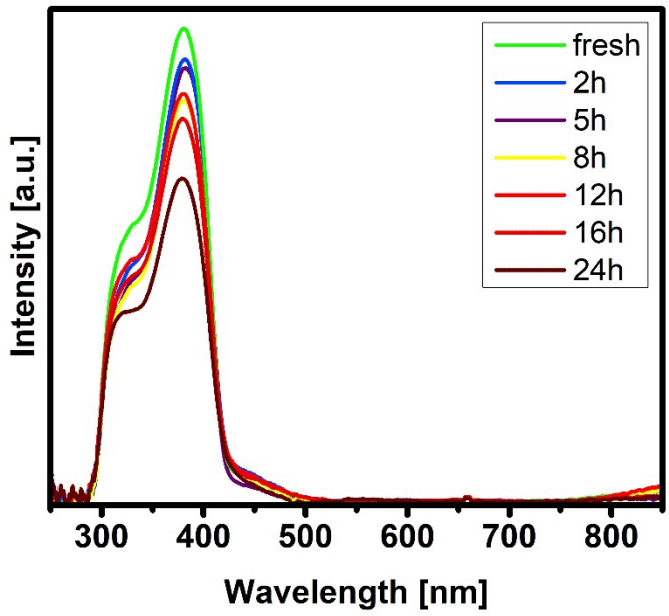


**Fig. S4.** UV-Vis spectra of neat and UV degraded PTTA films.

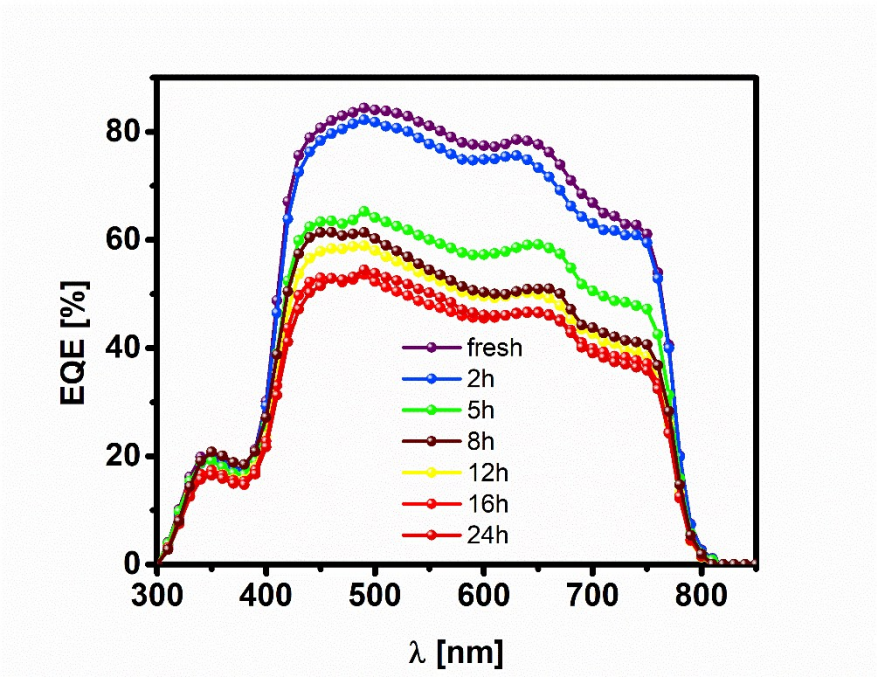


**Fig. S5.** External quantum efficiency of planar inverted perovskite solar cells (ITO/PTAA/MAPI/PCBM/PFN/Ag) subjected to various periods of UV exposure.

| *UV exposure* | Voc [V] | | Jsc [macm$^{-2}$] | | FF [%] | | PCE [%] | |
|---|---|---|---|---|---|---|---|---|
| | *forward* | *reverse* | *forward* | *reverse* | *forward* | *reverse* | *forward* | *reverse* |
| fresh | 0,98 | 0,97 | 17,09 | 17,53 | 70,57 | 70,6 | 13,10 | 13,25 |
| 2h | 0,99 | 0,99 | 16,53 | 16,23 | 67,11 | 68,59 | 12,12 | 12,18 |
| 5h | 0,99 | 1,00 | 14,81 | 14,48 | 68,79 | 69,97 | 11,17 | 11,15 |
| 8h | 1,01 | 1,01 | 15,69 | 15,31 | 63,79 | 65,9 | 11,14 | 11,18 |
| 12h | 1,01 | 1,01 | 13,92 | 13,55 | 66,13 | 68,15 | 10,13 | 10,14 |
| 16h | 0,99 | 0,99 | 13,59 | 13,21 | 59,53 | 61,23 | 8,80 | 8,87 |
| 24h | 0,95 | 0,94 | 11,84 | 11,51 | 48,80 | 57,86 | 6,87 | 6,04 |

**Table S1**. Reduction in power conversion efficiency of planar inverted perovskite solar cells (ITO/PTAA/MAPI/$PC_{60}BM$/PFN/Ag) as a result of UV induced degradation.

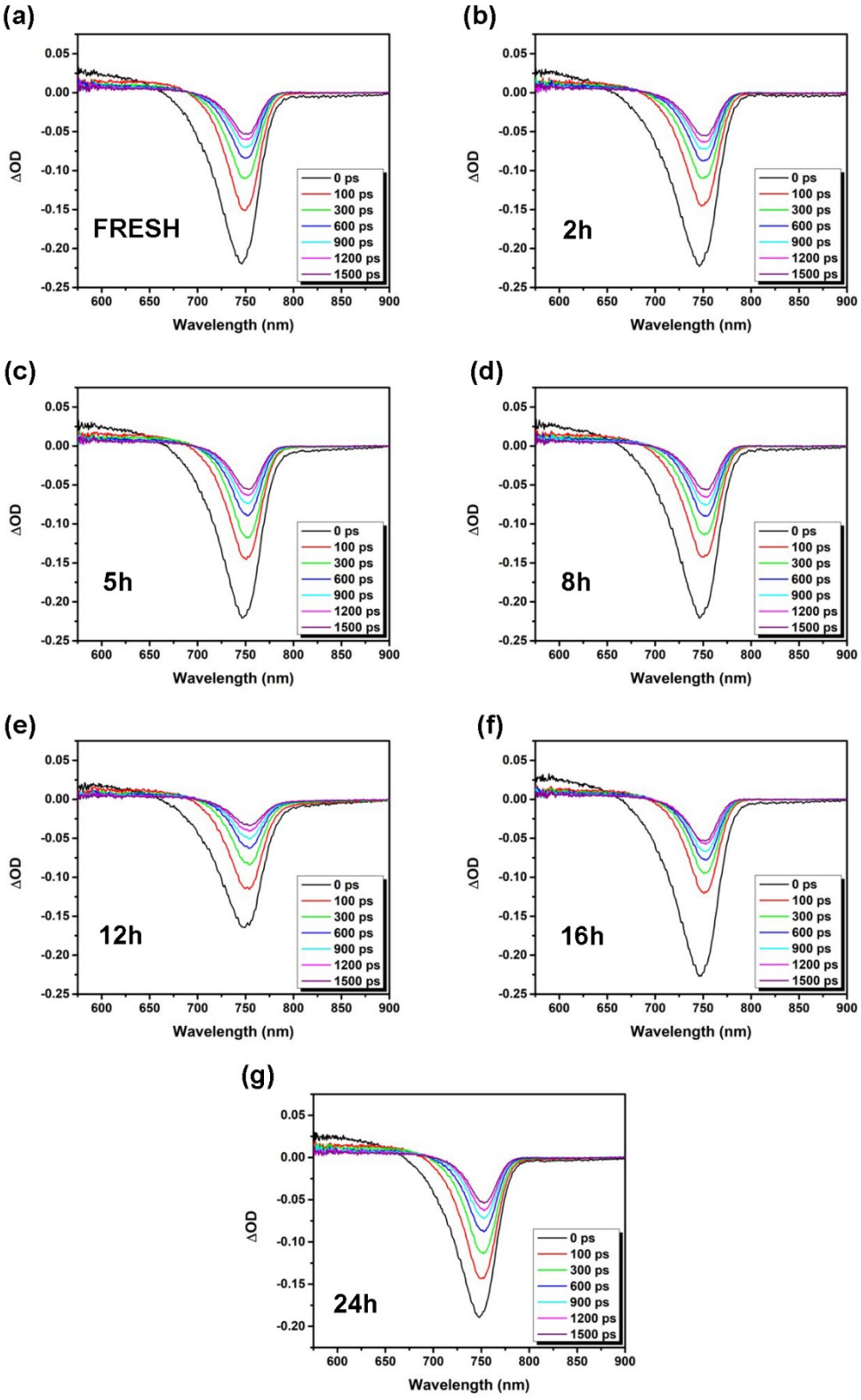


**Fig. S6**. Typical ΔOD vs wavelength graphs recorded by ultrafast TAS at various time delays for reference and UV degraded PTAA/MAPI bilayers.

| *UV exposure* | *λ (nm)* | *$k_3$ ($cm^6s^{-1}$) ± 0.5* | *$k_2$ ($cm^3s^{-1}$) ± 0.3* | *$k_1$ ($\mu s^{-1}$) ± 0.1* |
|---|---|---|---|---|
| fresh | 747 | $5.7 \cdot 10^{-13}$ | $9.8 \cdot 10^{-10}$ | $8.6 \cdot 10^{-7}$ |
| 2h | 747 | $8.5 \cdot 10^{-13}$ | $1.4 \cdot 10^{-9}$ | $1.1 \cdot 10^{-6}$ |
| 5h | 747 | $7.6 \cdot 10^{-13}$ | $1.3 \cdot 10^{-9}$ | $1.0 \cdot 10^{-6}$ |
| 8h | 747 | $7.7 \cdot 10^{-13}$ | $1.3 \cdot 10^{-9}$ | $1.0 \cdot 10^{-6}$ |
| 12h | 750 | $6.5 \cdot 10^{-13}$ | $1.1 \cdot 10^{-9}$ | $1.0 \cdot 10^{-6}$ |
| 16h | 747 | $8.0 \cdot 10^{-13}$ | $1.3 \cdot 10^{-9}$ | $1.1 \cdot 10^{-6}$ |
| 24h | 749 | $8.3 \cdot 10^{-13}$ | $1.8 \cdot 10^{-9}$ | $1.7 \cdot 10^{-6}$ |

**Table S2.** Recombination rate constants for the studied ITO/PTAA/MAPI architectures fitted according to polynomial correlation.

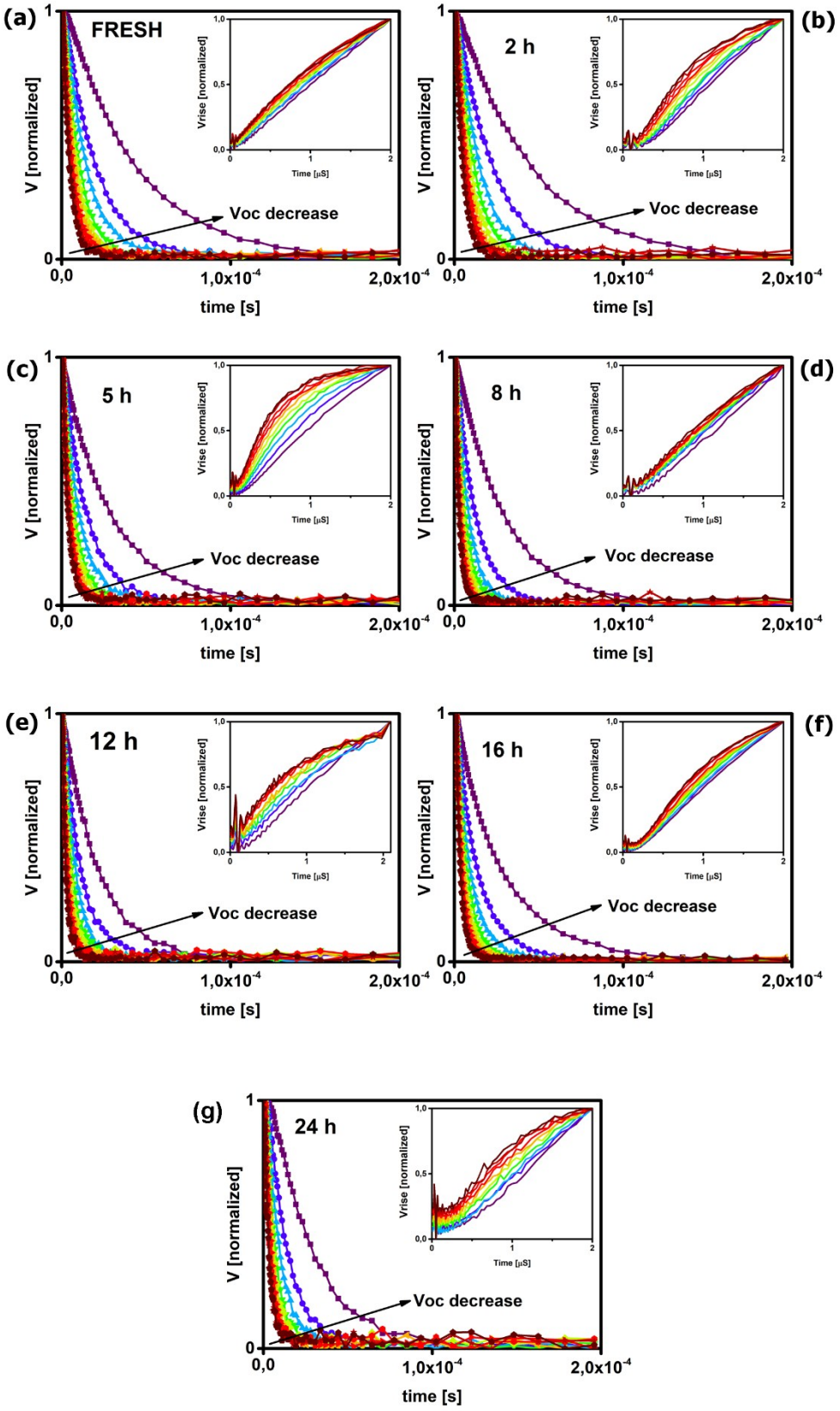


**Fig. S7.** Normalized small-perturbation transient photovoltage decay of ITO/PTAA/MAPI/Ag bilayer devices as a function of background bias recorded after UV stress and respective voltage rise responses (inset).

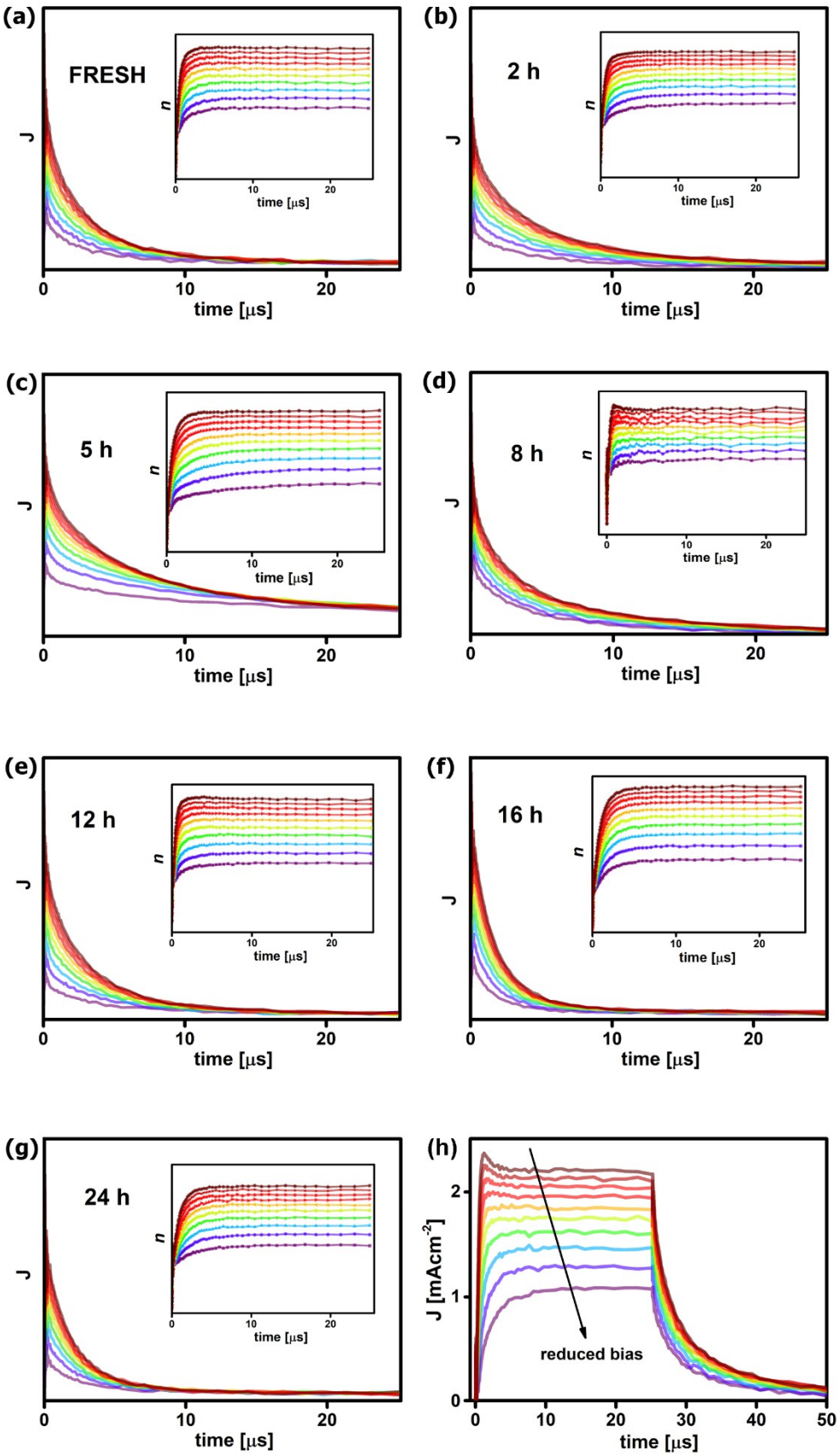


**Fig. S8.** (a-g) Photocurrent decay transients for bilayer devices at various UV exposure periods with respective collected charge over time (insets) and (h) absolute transient response of the fresh sample.

| *fresh* | | *2h* | | *5h* | | *8h* | | *12h* | | *16h* | | *24h* | |
|---|---|---|---|---|---|---|---|---|---|---|---|---|---|
| *Voc [V]* | *lifetime [µs]* | *Voc [V]* | *lifetime [µs]* | *Voc [V]* | *lifetime [µs]* | *Voc [V]* | *lifetime [µs]* | *Voc [V]* | *lifetime [µs]* | *Voc [V]* | *lifetime [µs]* | *Voc [V]* | *lifetime [µs]* |
| 0,40 | 42,23 | 0,39 | 49,28 | 0,39 | 29,75 | 0,33 | 29,49 | 0,32 | 22,69 | 0,34 | 16,38 | 0,32 | 17,15 |
| 0,42 | 21,50 | 0,41 | 23,87 | 0,42 | 12,80 | 0,35 | 15,26 | 0,33 | 11,36 | 0,35 | 8,39 | 0,33 | 12,32 |
| 0,43 | 15,41 | 0,42 | 15,87 | 0,44 | 8,44 | 0,36 | 10,19 | 0,34 | 8,41 | 0,35 | 6,19 | 0,33 | 9,23 |
| 0,44 | 11,24 | 0,43 | 12,27 | 0,44 | 6,49 | 0,37 | 7,83 | 0,34 | 6,16 | 0,36 | 4,77 | 0,33 | 8,02 |
| 0,44 | 9,45 | 0,44 | 10,10 | 0,45 | 5,33 | 0,38 | 6,52 | 0,35 | 5,04 | 0,36 | 3,88 | 0,33 | 5,93 |
| 0,45 | 7,81 | 0,44 | 8,51 | 0,45 | 4,46 | 0,38 | 5,41 | 0,35 | 4,26 | 0,36 | 3,33 | 0,34 | 4,70 |
| 0,45 | 6,73 | 0,44 | 7,44 | 0,46 | 3,79 | 0,38 | 5,54 | 0,35 | 3,73 | 0,37 | 2,89 | 0,34 | 3,83 |
| 0,45 | 6,19 | 0,45 | 7,31 | 0,46 | 3,43 | 0,39 | 4,44 | 0,35 | 3,28 | 0,37 | 2,57 | 0,34 | 3,26 |
| 0,46 | 5,58 | 0,45 | 5,85 | 0,46 | 2,99 | 0,39 | 3,83 | 0,36 | 2,93 | 0,37 | 2,28 | 0,34 | 2,87 |
| 0,46 | 4,85 | 0,45 | 5,11 | 0,46 | 2,83 | 0,39 | 4,10 | 0,36 | 2,65 | 0,37 | 2,10 | 0,35 | 2,41 |

**Table S3.** Charge recombination lifetimes extracted from PTAA/MAPI bilayer TPV transients as a function of background bias and UV exposure.

| *fresh* | | *2h* | | *5h* | | *8h* | |
|---|---|---|---|---|---|---|---|
| *current [mAcm$^{-2}$]* | *charge [nCcm$^{-2}$]* | *current [mAcm$^{-2}$]* | *charge [nCcm$^{-2}$]* | *current [mAcm$^{-2}$]* | *charge [nCcm$^{-2}$]* | *current [mAcm$^{-2}$]* | *charge [nCcm$^{-2}$]* |
| 0,51 | 6,58 | 1,29 | 7,04 | 0,51 | 3,93 | 0,37 | 4,18 |
| 0,81 | 8,00 | 1,50 | 7,61 | 0,84 | 5,23 | 0,85 | 5,56 |
| 1,09 | 9,97 | 1,72 | 7,42 | 1,11 | 5,68 | 1,14 | 6,47 |
| 1,30 | 9,92 | 1,94 | 7,96 | 1,39 | 6,30 | 1,62 | 7,31 |
| 1,57 | 11,24 | 2,16 | 9,27 | 1,66 | 7,50 | 2,04 | 8,14 |
| 1,69 | 12,05 | 2,36 | 10,59 | 1,89 | 8,31 | 2,39 | 8,52 |
| 1,92 | 13,19 | 2,50 | 11,35 | 2,05 | 8,29 | 2,86 | 9,72 |
| 2,03 | 12,83 | 2,66 | 12,96 | 2,29 | 9,45 | 3,10 | 10,03 |
| 2,20 | 13,73 | 2,81 | 13,11 | 2,40 | 9,72 | 3,32 | 10,49 |
| 2,31 | 13,81 | 2,98 | 13,84 | 2,63 | 10,18 | 3,48 | 10,58 |

| *12h* | | *16h* | | *24h* | |
|---|---|---|---|---|---|
| *current [mAcm$^{-2}$]* | *charge [nCcm$^{-2}$]* | *current [mAcm$^{-2}$]* | *charge [nCcm$^{-2}$]* | *current [mAcm$^{-2}$]* | *charge [nCcm$^{-2}$]* |
| 0,82 | 4,27 | 0,59 | 3,49 | 0,51 | 3,22 |
| 1,11 | 5,26 | 0,92 | 4,41 | 0,81 | 3,60 |
| 1,45 | 6,16 | 1,28 | 4,89 | 1,09 | 3,83 |
| 1,58 | 6,39 | 1,58 | 6,39 | 1,30 | 4,75 |
| 1,80 | 6,52 | 1,86 | 5,90 | 1,57 | 4,68 |
| 1,95 | 6,75 | 2,19 | 6,69 | 1,69 | 4,87 |
| 1,95 | 7,08 | 2,44 | 6,60 | 1,92 | 5,58 |
| 2,12 | 7,34 | 2,60 | 7,07 | 2,03 | 5,66 |
| 2,17 | 7,39 | 2,77 | 7,22 | 2,20 | 5,81 |
| 2,26 | 7,77 | 3,00 | 7,95 | 2,31 | 6,36 |

**Table S4.** Charge extraction parameters calculated from TPC transient recorded at variable current bias and UV degraded PTAA/MAPI bilayers.